

RSC Advances



This is an *Accepted Manuscript*, which has been through the Royal Society of Chemistry peer review process and has been accepted for publication.

Accepted Manuscripts are published online shortly after acceptance, before technical editing, formatting and proof reading. Using this free service, authors can make their results available to the community, in citable form, before we publish the edited article. This *Accepted Manuscript* will be replaced by the edited, formatted and paginated article as soon as this is available.

You can find more information about *Accepted Manuscripts* in the [Information for Authors](#).

Please note that technical editing may introduce minor changes to the text and/or graphics, which may alter content. The journal's standard [Terms & Conditions](#) and the [Ethical guidelines](#) still apply. In no event shall the Royal Society of Chemistry be held responsible for any errors or omissions in this *Accepted Manuscript* or any consequences arising from the use of any information it contains.

Impact of Lung Surfactant on Wettability and Cytotoxicity of Nanoparticles

Monica Ratoi^{1*}, Peter H. M. Hoet², Alison Crossley³ and Peter Dobson⁴

¹*Faculty of Engineering and Environment, University of Southampton, Highfield Campus, Southampton SO17 1BJ, UK, Email: m.ratoi@soton.ac.uk*

²*Laboratory of Pneumology, Unit for Lung Toxicity, K. U. Leuven, Herestraat 49, 3000 Leuven, Belgium*

³*Department of Materials, University of Oxford, UK*

⁴*Begbroke Science Park Directorate, University of Oxford, UK OX5 1PF*

**corresponding author*

Abstract

The importance of nanoparticle characterization for nanotoxicology has been extensively emphasized and it has been universally agreed that the most important parameters for characterizing nanomaterials are specific surface area and surface properties (chemistry, hydro-philicity/phobicity, charge etc). This study is proposing the use of enthalpy of wetting which depends on both specific surface area and surface properties, is easily measurable and proves to be highly relevant for predicting nanoparticles' dispersion state and their interaction with the lungs. It also shows the conditioning effect of the lung surfactant main component, DPPC on the surface of particles when used in concentrations which mimic pulmonary exposure more closely.

1. Introduction

1 **Currently, there is an increased interest in the potential toxicity effects associated with the inhalation**
2 **of nanoparticles (NPs). Beside size, one distinctive property of NPs is their tendency to agglomerate**
3 **and form weakly bound (by electrostatic and van der Waals forces) or sintered collections of primary**
4 **particles. The degree of NP agglomeration could influence their toxicity [1-5] and therefore, the state**
5 **of NP dispersion in the medium used to suspend them is an essential parameter required for the**
6 **interpretation of *in vitro* nanotoxicity studies. Different strategies to disperse NPs and a range of**
7 **biocompatible dispersion media have been investigated and proposed [4,6,7]. Researchers agreed that**
8 **is important that the dispersion medium mimics the components of the lung lining fluid essential to NP**
9 **dispersion and reported that their concentration affects not only the dispersion of NPs but also their**

1 toxicity [5,6]. It is therefore critical for the concentration of the dispersion agents to also mimic the *in*
2 *vivo pulmonary* conditions more closely.

3 Once inhaled, particles deposit in the hypophase where they adsorb the pulmonary surfactant on their
4 surface and then interact with the epithelial cells. The lung surfactant is produced by the *alveolar type*
5 *II cells* and coats the alveolar surfaces with a lining layer of lamellar liquid crystals (10-20 nm thick)
6 formed by bilayers of long-chain phospholipids (90 wt%) stabilized by specific proteins (SP-C and SP-
7 B,10 wt%) in the aqueous media [8,9,10,11]. The lamellar bodies maintain the function of the lungs:
8 facilitation of gas exchange and prevention of alveoli collapse by reducing the lung air interfacial
9 tension [12]. Dipalmitoylphosphatidylcholine (DPPC) together with proteins SP-B and SP-C are the main
10 contributors to the surface activity of the pulmonary surfactant [13] and a large number of studies used
11 DPPC as a surrogate of lung surfactant [1,4-6,14-24].

12 Through their adsorption on solid surfaces, surfactants can modify their wettability [25, 26].
13 Wettability of NPs is particularly important for understanding nanoparticle aggregation, dissolution and
14 bioaccumulation [27]. Surface wettability, the degree to which a fluid spreads on a solid surface,
15 depends on the nature of the surface and the fluid involved. Used in concentrations higher than the
16 critical micelle concentration, surfactants adsorb as monolayers on hydrophobic surfaces/particles (i.e.
17 carbon, polymers, etc.) and form bilayers on hydrophilic ones (i.e. metal, metal oxides, glass, ceramics)
18 [28, 29, 30]. This is also the case of the zwitterionic surface agent DPPC which in high concentrations,
19 adsorbs on hydrophilic surfaces as multiple bilayers (5-6 nm in thickness) which trap a 2 nm layer of
20 water in between them [31]. The complete DPPC bilayers expose the hydrophilic moieties and provide
21 polar, water 'wetable' surfaces.

22 The lamellar liquid crystals formed by the lung surfactant in hypophase contain abundant amounts of
23 DPPC and enables adsorption of complete DPPC bilayers on hydrophilic particles and monolayers on
24 hydrophobic particles. Regardless of the wettability of particles, through its adsorption on their
25 surface, DPPC renders them hydrophilic (Figure 1) and consequently influences their dispersability and
26 surface charge.

27 Numerous studies investigated the dispersion and toxicity of fine and ultrafine particles in DPPC or BAL
28 (brochoalveolar lavage) aqueous media. The concentration of the DPPC/ BAL varied widely and
29 generated potentially conflicting outcomes of both, dispersion state and toxicity of particles as it has
30 been emphasized by several authors [1,4, 7, 32]. Wallace and al. [6, 14- 22] investigated and revealed
31 the importance of employing high DPPC concentrations in particle toxicity studies. Other authors
32 [5,23,33] who followed Wallace's recommendation reported similar toxicology results. Despite the
33 evidence of these reported findings, the majority of published research used diluted DPPC/BAL
34 dispersion media which did not promote a complete phospholipid mono (on hydrophobic NPs) or

1 **bilayer (hydrophilic surface) coverage. An incomplete DPPC monolayer/bilayer coverage alters the**
 2 **wettability of the particles and it can convert hydrophilic particles into hydrophobic. This explains the**
 3 **outcomes of many studies which reported that DPPC/ BAL dispersion media led to particle**
 4 **agglomeration, sedimentation and various contradictory toxicity effects.**

5 Wetting is primarily an enthalpy driven process and the *enthalpy of wetting* is directly related to
 6 parameters which have been linked to toxicity of NPs such as: surface area, surface charge, chemistry and
 7 solubility and has the potential to be a valuable characterization parameter [34,35].

8 This study has investigated how DPPC adsorbs on the titania P25 NPs and influences their dispersion and
 9 cytotoxicity. It also introduces a novel characterization parameter, *the enthalpy of wetting* of NPs and
 10 explores its potential to predict the NPs dispersion and interaction with biological systems.

2. Materials and methods

2.1. Test particles

11 Aeroxide P25 titania NPs were supplied by Evonik Industries AG. The primary particle size, specific surface
 12 area and tamped density supplied by the manufacturer in the product information sheet, are listed in
 13 Table 1. The phase composition also shown in Table 1 was calculated from XRD analysis. The pH of point
 14 of zero charge (PZC) of titania P25 NPs measured in deionized water (DI) was 6.7.

Table 1: P25 Titania NP parameters

	Mean primary particle size diameter (nm)	BET Specific surface area (m ² g ⁻¹)	Tamped density (g l ⁻¹)	Composition (wt.%)
Aeroxide P25	21	50±15	approx. 130	80 % anatase & 20 % rutile

2.2. DPPC coating of P25 titania nanoparticles

15 **1,2-dipalmitoyl- *sn*-glycero-3-phosphocholine (DPPC) ≥99% (M=734.04) was purchased from Sigma**
 16 **Aldrich, UK.**
 17 **The coating of the NPs with DPPC followed the procedure proposed by Wallace and collaborators [6].**
 18 **The surfactant dispersion was prepared at 37 °C by ultrasonically mixing DPPC in physiological saline**
 19 **(PSS) at 1.25 mg DPPC/1 ml PSS. Although surface active, lecithin has very low solubility in water.**
 20 **Titania P25 NPs were ultrasonically mixed into the surfactant dispersions in 1 mg NPs/1.25 mg DPPC/1**
 21 **ml PSS and gently stirred in an incubator at 37 °C for one hour. NPs were centrifuged (4025 G-force)**
 22 **and the supernatant decanted. Additional DI water was added to the pellet and the centrifuge-washing**

1 step repeated three times. The DPPC coated P25 NPs were freeze-dried to a powder. This procedure
2 ensured that the titania NPs were fully covered in lipid but only a *single bilayer* remained as showed by
3 the Raman analysis and wettability results.

4 To investigate the dispersability of the pristine and DPPC coated NPs in DI water (Millipore Nanopure
5 Water), the dispersions were prepared in three concentrations: C1=1000 µg/ml, C2=100 µg/ml and
6 C3=10 µg/ml. NP dispersions in C1 were sonicated for 15 minutes using a bath sonicator before
7 dilution to C2 and C3. Vortexing at maximum power for 15 seconds was employed before dilutions and
8 the measurement of particle size distribution and surface charge. The pH of the NP dispersions in DI
9 water was approximately 7.

2.3. Characterization of NP dry powders

2.3.1. BET specific surface area

10 Specific surface area measurements have been carried out on a Micromeritics Gemini V BET surface
11 area analyser. Prior to measurements, samples of 150-200 mg have been degassed in nitrogen
12 atmosphere overnight at 25 °C. Two measurements were carried out for each sample.

2.3.2. Raman spectroscopy

13 Raman spectroscopy analysis was performed using a microRaman spectrograph (Horiba LabRAM Aramis
14 integrated confocal system 460 mm focal length) with an internal He-Ne laser 633 nm and 20 mW output
15 power. The laser source was focused on the samples through a long working distance 50x objective to a
16 spot diameter of 2 µm. The acquisition time for Raman spectra was 10-20 minutes depending on the
17 strength of the Raman signals, until a satisfactory signal-to-noise ratio was achieved.

2.3.3. Microcalorimetry

18 The heat of wetting/dewetting of NPs was measured with the TA Instruments Relative Humidity (RH)
19 Perfusion Microcalorimeter equipped with the TAM III thermostat. The microcalorimeter is a heat-flow
20 calorimeter of the twin-type which uses a 20 ml ampoule. It was preferred to the nanocalorimeter
21 because the ampoule size permits a larger contact area of the water/solvent vapours with the
22 nanopowder and can therefore reveal smaller differences in the wettability of samples.

23 The RH was kept constant at 10% until a stable heat flow was reached (signal within the range of -1 to
24 +1 µW). The RH was then increased in a linear ramp from 10% to 90% over the following 10 hours and
25 maintained at 90% for 10 hours. During the increase of humidity, the moisture interacts with the
26 sample and produces a heat flow, called *heat of wetting*. The TAM III was housed in a thermostatic

1 room maintained at $25\pm 1^\circ\text{C}$ and it was calibrated with empty stainless steel ampoules before the
2 experiments. The measurements were carried out on 35-50 mg of samples and were repeated twice.

2.4. Characterization of NP dispersions

3 2.4.1. Particle size distribution and charge

4 The hydrodynamic size distributions of the NP dispersions were measured with the Malvern Zetasizer
5 and CPS Disc Centrifuge (*CPS Disc Centrifuge Model DC24000*, CPS Instruments, Europe) which are
6 Dynamic Light Scattering (DLS) techniques. In the CPS Centrifuge, dispersion samples of 300 μl were
7 analyzed at 12000 RPM. The *ZetaSizer Nano ZS* (Malvern Instruments, UK) equipped with MPT-2
8 Multipurpose Titrator was employed for measurements of hydrodynamic particle size distribution,
9 surface charge (zeta potential) and point of zero charge (PZC).

10 The titania dispersions were prepared in DI water rather than other biological media to be able to
11 compare the particle size and surface charge results with the wettability values (heat of
12 wetting/dewetting of water vapours). Prior to the size and zeta potential measurements, titania
13 dispersions were sonicated for 15 minutes using a bath sonicator and vortexed for 15 seconds before
14 each dilution. All measurements were carried out at 25°C . Repeatability of all hydrodynamic size and
15 zeta potential was checked more than three times.

2.5. Cell culture

16 A549 cells from a human lung adenocarcinoma with alveolar type II phenotype were obtained from
17 Salisbury, UK (ECACC #8601284). Cells were cultured in RPMI 1640 with 25 mM HEPES and Glutamax
18 (Gibco #72400-021), 10 % FBS (ATCC #30-2021), 1% Penicillin-streptomycin (100x Gibco #15140-122),
19 0.5% Fungizone (100x Gibco #15290-018) and Trypsin-EDTA (10x Gibco #15400-054) in a humidified
20 atmosphere at 37°C .

21 A cytotoxicity dose–response curve was created for the different nanoparticles, in the presence or
22 absence of DPPC, using the thiazolyl blue tetrazolium bromide (MTT) or lactate dehydrogenase (LDH)
23 assay. The cells were seeded at a density of 100×10^3 cells/ cm^3 and medium was removed 24 hours later.
24 The cultures were exposed to 3.3, 10, 33, 100, 333, 1000, 3333 μg nanoparticles/ml. DPPC alone was
25 dosed at a 10 fold lower concentration [36]. In these experiments, controls and negative controls were
26 included as described in [36,37].

2.5.1. MTT assay

1 After 24 h of exposure, the medium was removed and cells were rinsed with HBSS. The MTT solution (0.5
2 mg/ml MTT in HBSS) was added for 3 hours. Thereafter, the MTT solution was removed, and 100 μ l of
3 DMSO was added. The optical density was read at 550 nm with 655 nm as reference wavelength, using a
4 microplate reader (Bio-Rad). Cells not incubated with nanoparticles and/or DPPC served as 100% viability
5 control (*n=6 wells in 2 separate experiments*).

2.5.2. LDH assay

6 Cells integrity was assessed by determining the percentage of LDH retained by the cellular layer. For LDH
7 assay, after incubation with particles, the medium was removed; the adherent cells were washed twice
8 with PBS (200 mL) and then lysed using Triton-X (0.2%). The LDH activity of the medium (LDH medium)
9 and the cell lysate (LDH cells) were determined spectrophotometrically monitoring the reduction of
10 pyruvate. Cell viability was calculated according to the formula:

11 % viability = $[\text{LDH}_{\text{cells}} / (\text{LDH}_{\text{cells}} + \text{LDH}_{\text{medium}})] \times 100$ (*n=6 wells in 2 separate experiments*).

3. Results and discussion

3.1. Adsorption of lung surfactant on NPs

12 **The surface of P25 titania NPs dispersed in water is generally covered by hydroxyl groups [38]. Having a**
13 **polar surface, titania NPs are hydrophilic and will adsorb at least a bilayer of DPPC on their surface. In**
14 **the current study, the calculated amount of DPPC necessary to cover with a complete bilayer 1 mg P25**
15 **titania NPs was 0.32 mg (considering the surface area per DPPC molecule of 40 \AA^2 and the specific**
16 **surface area of P25 NPs of 52.58 m^2/g). To ensure the DPPC concentration was sufficiently high to form**
17 **a complete bilayer on NPs, we started with the amount ratio recommended by Wallace [6] of 2.50 mg**
18 **DPPC/1 ml PSS/1 mg NPs.**

19 **This DPPC amount was difficult to disperse in PSS and it was diluted down to 1.25 mg DPPC/1 ml PSS. 1**
20 **mg NPs was mixed in the phospholipid dispersion which contained four times the DPPC amount**
21 **necessary for complete bilayer coverage. The excess DPPC was removed by multiple rinsing with DI**
22 **water.**

23 The recommendations of Wallace and al. for the DPPC/NPs wt. ratio were based on data from
24 unpublished investigations. In earlier published studies of microsized silica particles, Wallace employed
25 the wet phosphate assay to quantify the particle uptake of DPPC from PSS dispersions at 37 $^{\circ}\text{C}$ over a
26 range of DPPC dispersion concentrations. Two types of silicate particles, quartz and kaolin with specific
27 surface area values of 4 m^2/g and 13 m^2/g respectively were found to adsorb 50-60 mg and 150 mg
28 lecithin/gram as multilayers [15,19].

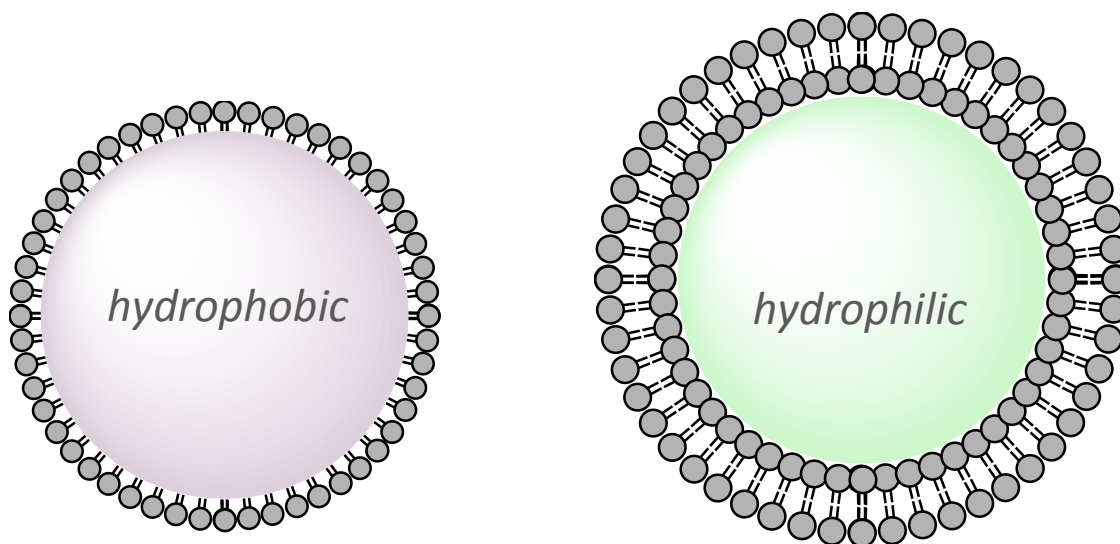


Fig. 1. Schematics of phospholipid adsorption as a monolayer on hydrophobic surface NPs (i.e. polymers, etc.) and as bilayers on hydrophilic surface NPs (i.e. metals, metalloids, oxides, etc.). The phospholipid coating renders the surface of all NPs hydrophilic (water wettable) when used in concentrations which mimic *in vivo* conditions.

1 The 2.50 mg DPPC/1 mg NPs wt. ratio recommended by Wallace [6] is indeed high but it is the amount
 2 required to assure a complete bilayer coverage of NPs such as polar (i.e. surface functionalized) CNTs
 3 because of their very high specific surface area (i.e. 2.2-3 mg DPPC are necessary to achieve complete
 4 bilayer coverage of 1 mg CNT with $S_{SA}=490 \text{ m}^2/\text{g}$). The excess DPPC can be rinsed off from the coated
 5 NPs because the complete monolayer/bilayer is stable to water rinsing [6, 39].

6 The presence of the DPPC bilayer coating on NPs was tested with Raman spectroscopy. The Raman
 7 spectra for the DPPC coated P25 NPs, P25 NPs and DPPC powder are shown in Figure 2.

8 For DPPC powder, a representative spectrum similar to other published spectra [40] is shown in Figure 3
 9 with band assignments. Spectral peaks can be found in the fingerprint region ($600\text{-}1800 \text{ cm}^{-1}$) associated
 10 with choline symmetric stretch (718 cm^{-1}) and the lipid hydrocarbon acyl chains: ($1060, 1100, \text{ and } 1128$
 11 cm^{-1}) but the most intense bands in the spectrum are the C-H stretching region ($2800\text{-}3100 \text{ cm}^{-1}$). The
 12 methylene vibrations at $2845, 2880, 2930$ are sensitive to conformational changes as well as intermolecular
 13 interactions of the alkyl chains of lipids and therefore has been much research focused on their
 14 interpretation. The Raman spectra for DPPC-P25 NP as compared to DPPC powder show a change in
 15 intensity ratio for the $2850/2880 \text{ cm}^{-1}$ bands. The intensity ratio, I_{2880}/I_{2845} derived from these spectra,
 16 serves as an index of the strength of the lateral interchain packing interactions in the bilayer [41]. The

- 1 intensity ratio value for DPPC-P25 is 1.04 similar to that found by other researchers for supported DPPC
- 2 bilayers on SiO₂ NPs with a diameter of 30-40 nm [42].

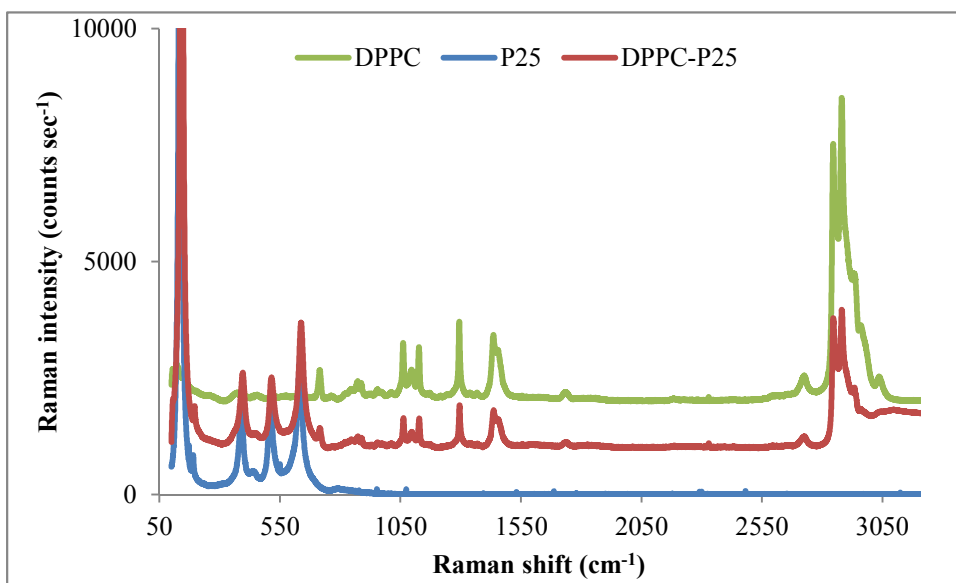


Figure 2. Raman Spectra for P25 NPs, DPPC coated P25 NPs and DPPC powder

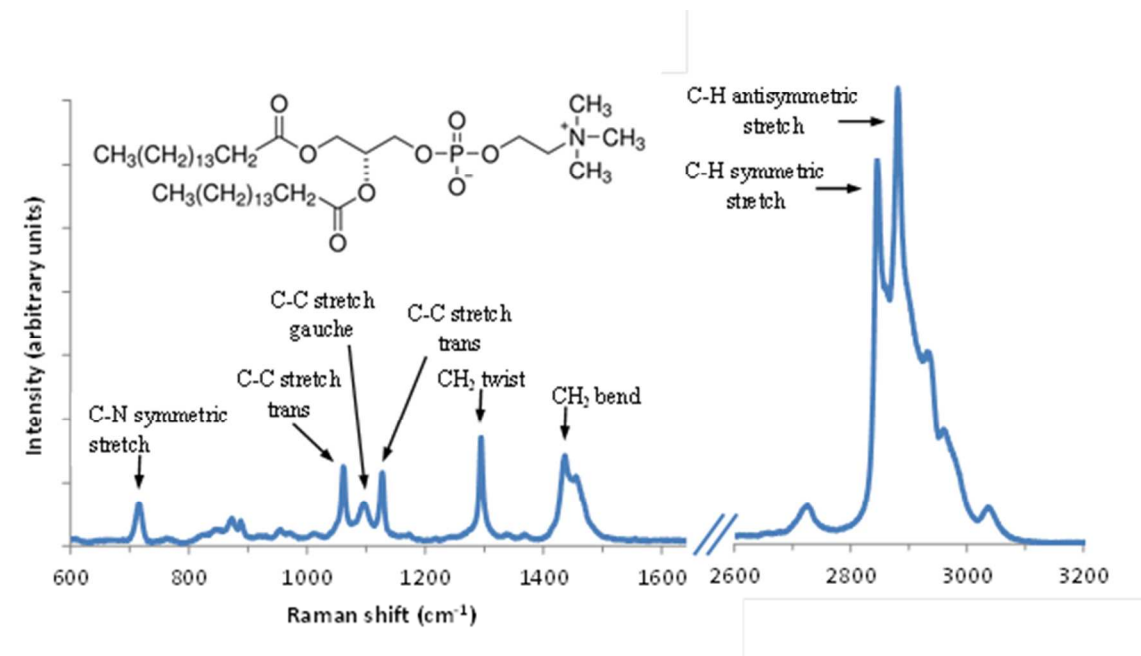


Figure 3. Raman Spectrum of DPPC powder, showing structure of DPPC and band assignments

3.2. Effect of DPPC coating on wettability, dispersability and surface charge of NPs

1 For solid surfaces, the most popular parameter used to describe wettability is the contact angle. For
2 powders, two main methods have been traditionally used for determining the contact angle:
3 measurements on a compacted powder surface and of the penetration into loosely packed beds but
4 because of the irregular geometry of the systems both present problems [43,44]. The penetration
5 experiment uses the Washburn equation which has been shown to be flawed [45] and in the case of
6 compressed powder, the effect of compression affects the values of the contact angle. A newer, simple
7 approach was proposed by Shanker [46], in which the powder is glued to an inert support but this method
8 also has its practical drawbacks. Recently, two novel techniques for determination of contact angles of
9 NPs were proposed: multi-angle single-wavelength ellipsometry [47] and freeze-fracture shadow-casting
10 cryo-scanning electromicroscopy [48]. These methods also have shortcomings and are yet at the
11 experimental stage.

12 *Isothermal microcalorimetry*, which measures the heat changes associated with the wetting process, is a
13 sensitive and straightforward way to measure wettability of powders. Measurements are carried under
14 controlled environmental conditions and can also be carried out for hydrophobic powders. Generally, the
15 heats of immersion in water are high for the hydrophilic surfaces (indicating a strong interaction with
16 water molecules) and low for the hydrophobic ones [49].

17 Enthalpy of wetting is the heat of wetting (measured with isothermal calorimetry) divided by the specific
18 surface area of the powder and depends on the nature of the surface (chemistry and roughness) and the
19 dissolution (solubility) in the wetting fluid. For a number of inorganic oxides, a linear relation has been
20 found to exist between the heat of wetting and the point of zero charge (PZC) [34,35].

21 Figure 4 shows the thermograms for wetting and de-wetting by water of the surface of P25 and DPPC
22 coated P25 NPs. The humidity has been increased and decreased from 10 to 90 %.

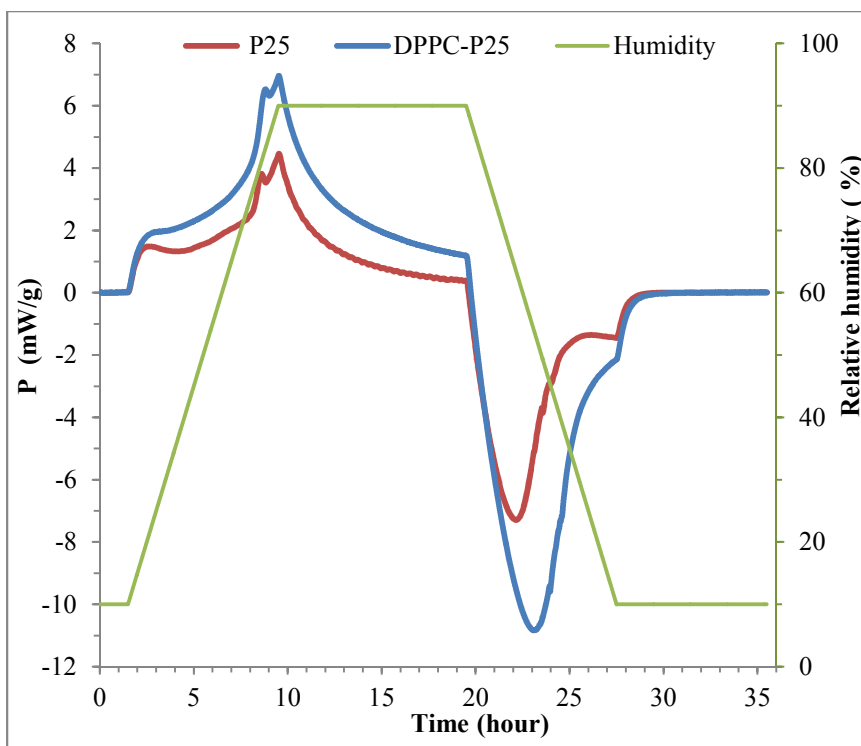


Figure 4. Thermograms for wetting/dewetting of P25 and DPPC coated P25 NPs

- 1 Table 2 shows the measured values of the heat of wetting/de-wetting with water and the BET specific
- 2 surface area of the P25 and DPPC coated P25. All measurements were carried out at 25 °C and were
- 3 repeated at least once.

Table 2: Surface area, heat and enthalpy of⁴
wetting of P25 and DPPC coated P25 NPs

5

	P25	DPPC-P25
BET Specific Surface Area (m²/g)	52.58 ±3	14.54 ±1 ₇
Heat of Wetting/Dewetting g -Δh_w/Δh_{dw} (mJ/g)	91.8/91.99 ±2	179.5/173.6 ±1
Enthalpy of Wetting -ΔH_w (mJ/m²)	1.7	12.3 ¹⁰

1 Both samples show an exothermic heat flow (negative heat of wetting) during moisture adsorption
2 (increasing humidity) and endothermic heat flow during moisture desorption which indicates that the
3 surfaces of NPs are hydrophilic. The heat of immersion enthalpy (absolute value) and the surface free
4 energy increase with the hydrophilicity of the sample. By integrating from a 10% RH equilibrium
5 through to 90% RH and reversing to 10% RH equilibrium there is a significant difference in the moisture
6 interaction (wettability) between samples. The DPPC-NPs have larger negative values of heat than the
7 non-coated NPs which indicates that the DPPC coating increased the hydrophilicity of P25 NPs.

8 Published work which measured the surface free energy and its components to study wettability of spin
9 coated DPPC applied on hydrophilic materials (slides of glass, silica and mica) reported similar findings.
10 The concentration of the DPPC was found to exert a major influence on the wettability of the coating.
11 The hydrophilic character of the coating decreased when DPPC concentrations were up to 0.5 mg/ml
12 and it increased and levelled off when 2-2.5 mg/ml was used. The advancing contact angle of water in
13 the second case was $10 \pm 2.6^\circ$ which means that water almost completely spreads on the DPPC
14 coating [50].

15 The enthalpy of wetting is calculated by dividing the measured heat of wetting by the BET specific
16 surface area.

17 The measured BET specific surface areas for the pristine and DPPC coated P25 NPs are shown in Table 2.
18 It is known that the surface area and porosity of NPs can change as a result of adsorption of
19 biomolecules or agglomeration [27]. Our results show that the surface area of DPPC-P25 NPs has been
20 substantially decreased by the DPPC bilayer adsorption on P25 NPs. BET surface area measurements
21 were also carried out on pristine and DPPC coated *rutile* titania NPs (our unpublished data) and a
22 similar degree of reduction in specific surface area was recorded. The particle size distribution data
23 which will be presented later showed that the agglomeration of the NPs did not contribute to the size
24 decrease because the particle size distributions of DPPC-P25 dispersion in DI water indicate much lower
25 average sizes and polydispersity than the pristine P25 NPs. Therefore, we considered that this decrease
26 in specific surface area can be due to two main factors. First, in the calculation of the specific areas of
27 both, the pristine and DPPC coated P25 NPs, the same tapped density value of 1.3 g/cm^3 (supplied by
28 the manufacturer) was used because the tapped density value for DPPC-P25 NPs wasn't available.

29 However, the DPPC coating increases the size of NPs by 30% (21 nm + 10 nm DPPC bilayer coating) and
30 consequently, the density of the DPPC-P25 NPs must be smaller. For example, if the density of a P25 NP
31 is $\rho_{\text{P25}} = 3.8 \text{ g/cm}^3$ and the density of the DPPC coating $\rho_{\text{DPPC}} = 1.03 \text{ g/cm}^3$, the density of a DPPC-P25 NP
32 will be reduced to half the density value of P25 NP ($\rho_{\text{DPPC-P25}} \cong 1.9$). This reduction of the DPPC-P25 NP
33 density implies that the measured BET specific surface area is actually twice the value shown in Table 3.

1 The second factor which could contribute to the large decrease in specific surface area of DPPC-P25 NPs
 2 is the potential of the coating to cover/block the pores present on the surface of the P25 NPs. BET
 3 surface area depends on the amount of N_2 gas adsorbed in the pores of the NPs surface. P25 NPs have
 4 pore volume of $0.25 \text{ cm}^3/\text{g}$ and pore size of 17.5 nm [51] and it is mesoporous according to IUPAC
 5 classification (size of pores 2-50 nm). By covering the pores and the adsorption sites on the P25 NPs,
 6 the DPPC coating can reduce the roughness and therefore, the specific surface area of NPs.
 7 The hydrophilicity (water wettability) and the surface charge of NPs are important factors which
 8 influence their dispersability and colloidal stability in water. To further investigate the effect of the
 9 DPPC coating on the P25 NPs, dispersions of NPs in DI water were prepared in a range of three
 10 concentrations relevant to the toxicology studies. The surface charge of NPs and the size distribution of
 11 the dispersions were measured with the Zetasizer and the CPS centrifuge.

Table 3. Surface charge of NP dispersions in
 DI water in three concentrations

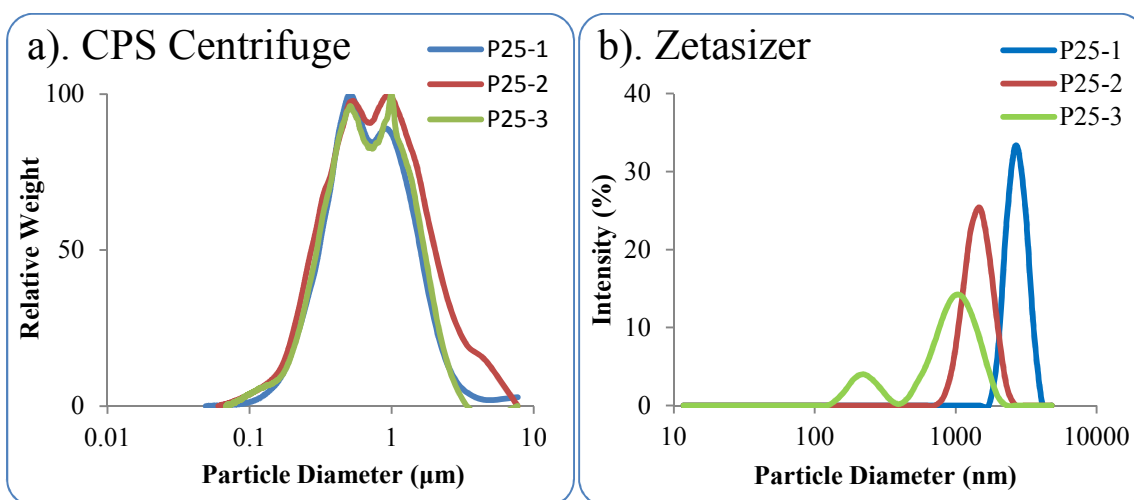
	Concentration ($\mu\text{g}/\text{ml}$)	Av. Zeta Potential at 22°C (mV)
P25	$C_1 = 1000$	-0.5
	$C_2 = 100$	-21.1
	$C_3 = 10$	-24.2
DPPC-P25	$C_1 = 1000$	-29.0
	$C_2 = 100$	-35.1
	$C_3 = 10$	-39.4

19 The zeta potential results listed in Table 3 indicate that the DPPC-P25 NPs have the largest measured
 20 negative surface charge values in all three concentrations. The pH of the dispersions was
 21 approximately 7 and all zeta potential values are at or above the threshold value for stable dispersions
 22 (-30 mV).

23 Figures 5a and 5c show the particle size distribution measured with the CPS centrifuge for the pristine
 24 and DPPC coated P25 dispersions in three concentrations. The CPS centrifuge results shown in Figure 5a
 25 indicate that P25 dispersions in DI water were broadly polydispersed (PSD spreading between 0.08-5
 26 μm). The results measured with Malvern Zetasizer (Figure 5b) were not qualitatively acceptable
 27 because of the polydispersity of the samples.

28 The DPPC-P25 NP dispersions measured with CPS centrifuge (Figure 5c) and Malvern Zetasizer (Figure
 29 5d) show low average sizes and narrow distributions for all three concentrations tested. In this case the
 30 Malvern Zetasizer results were qualitatively acceptable and the size distribution was more similar to

1 that measured by the CPS centrifuge. Both instruments measure the dispersions hydrodynamic
2 diameter which is controlled by NPs agglomeration (function of zeta potential and ionic strength of
3 dispersion media) in the aqueous system but also a strong function of primary particle size. Published
4 research studies [38] which also employed the Malvern Zetasizer to investigate titania NP dispersions in
5 DI water showed that even when the dispersions were stable (the zeta potential was 30 mV), the
6 measured average hydrodynamic diameter was much larger than the primary particle size (the
7 measured average hydrodynamic diameter of NPs with primary size of 6 nm was 67 nm).
8 Figures 5e and 5f compare PSDs measured with the CPS Centrifuge and Malvern Zetasizer of 0.1 mg/ml
9 (C2) P25 and DPPC-P25 dispersions in DI water. The DPPC-P25 dispersion has a small average particle
10 size and a narrow distribution while the P25 dispersion has large average particle size (forms large
11 aggregates) and is broadly polydispersed. The Zetasizer distribution results for the P25 dispersions did
12 not meet the quality criteria because the polydispersity index was too high (the size distribution for C2
13 dispersion was plotted in figure 5f for comparison only).



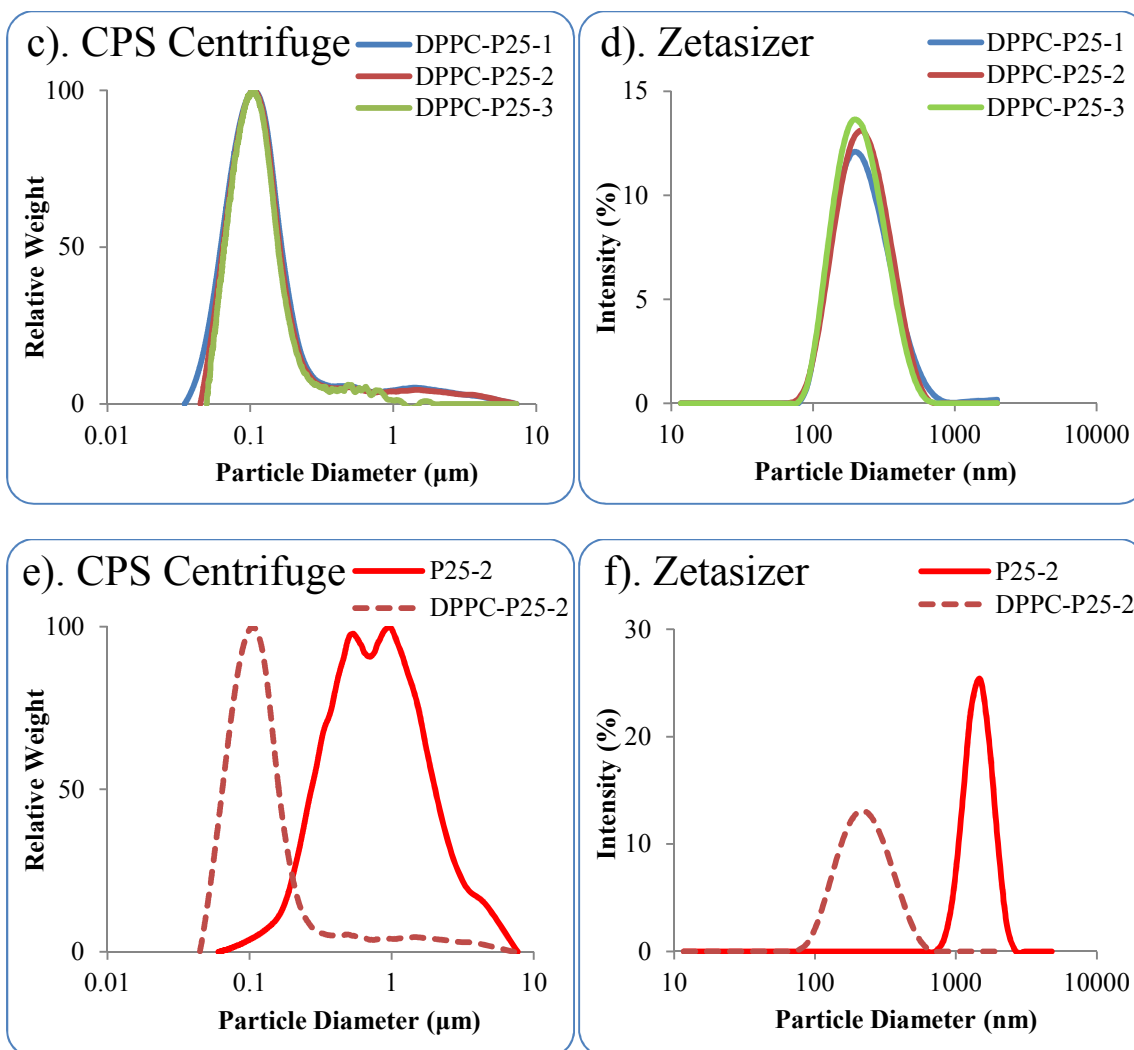


Figure 5. Particle size distribution of NP dispersions in DI water a). P25 C1=1, C2=0.1, C3=0.01 mg/ml dispersions measured with CPS Centrifuge, b). P25 C1=1, C2=0.1, C3=0.01 mg/ml dispersions measured with Malvern Zetasizer, c) DPPC-P25 C1=1, C2=0.1, C3=0.01 mg/ml dispersions measured with CPS Centrifuge, d). DPPC-P25 C1=1, C2=0.1, C3=0.01 mg/ml dispersions measured with Malvern Zetasizer, e). P25 and DPPC-P25 C2=0.1 mg/ml dispersions measured with CPS centrifuge and f). P25 and DPPC-P25 C2=0.1 mg/ml dispersions measured with Malvern Zetasizer

- 1 The particle size distribution and zeta potential results indicate that the DPPC coating increases the
- 2 surface charge and reduces both, the average hydrodynamic diameter and polydispersity of the P25 NP
- 3 dispersions, therefore generating a more stable NP dispersion. These results correlate very well with
- 4 the heat of wetting values which also show a large increase in the wettability of P25 NPs when coated
- 5 with a complete bilayer of DPPC.

3.3. Effect of DPPC coating on cytotoxicity of NPs

1 **Figure 6 a and b show the 24 hours A549 cell viability versus nanoparticle concentration and the SDs of**
 2 **the pristine and DPPC coated P25 using the LDH and MTT assays.**

3 The results show the effect of the DPPC coating on the NP cytotoxicity. One way Anova reveals that in the
 4 LDH and MTT assays, P25 NPs are significant different from DPPC-P25.

5 The toxicity of DPPC-P25 NPs is reduced in the entire concentration range tested and reached 25% (75%
 6 viability) at high NP concentrations (above 100 $\mu\text{g cm}^{-1}$). For the DPPC-P25 NPs there is a slight downshift
 7 in the viability curve for the top two concentrations but these doses are very high as the highest standard
 8 dose is typically 333 $\mu\text{g cm}^{-2}$.

9

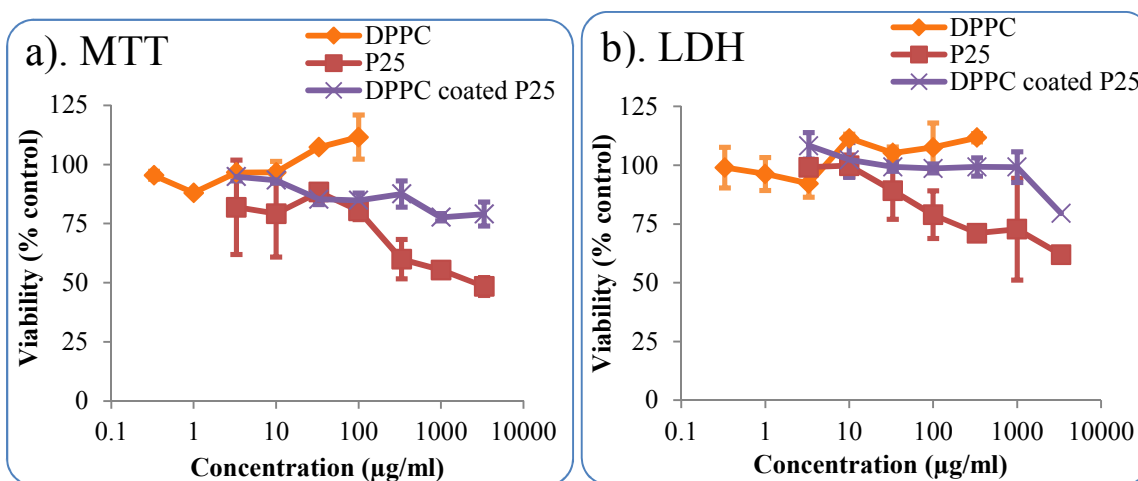


Figure 6. A549 cells viability exposed to pristine and DPPC coated P25 NPs a). MTT assay and b). LDH assay

10 Several studies employed DPPC concentration which enabled the complete coverage of NPs and
 11 demonstrated the protective effects of lung surfactant coating on toxic particles (silica etc.). Wallace and
 12 al. [15] showed that the DPPC treated quartz and kaolin particles incubated for 1 hour with erythrocytes
 13 suppressed the hemolytic strength of particles to background levels. Studies on pulmonary alveolar
 14 macrophages showed the DPPC fully suppressed silica NPs prompt cytotoxic, apoptotic, necrotic and
 15 genotoxic activity for 3 days [15,16,33,52] The interaction between DPPC and different types of silica
 16 dust has been suggested to modulate the toxicity of the particles through the molecular orientation of the
 17 adsorbed DPPC molecules. This may account for differences in pulmonary disease abnormalities [21]. The

1 artificial surfactant Survanta (FDA approved pulmonary surfactant extracted from minced cow lung with
2 additional DPPC, palmitic acid and tripalmitin) protected alveolar macrophages *in vitro* and reduced lung
3 injury *in vivo* without affecting neutrophil influx [53]. In the special case of crysotile asbestos, the
4 prophylactic effect of the DPPC coating was found ineffective at inhibiting its toxicity [33] despite the
5 reported ability to adsorb on its surface [54]. This finding reveals that the toxicity of crysotile asbestos
6 may thus depend on parameters other than the surface properties such as the shape of particles.

7 The protective effect against toxic particle induced lung-damage is only temporary as research showed
8 that subsequent removal of the prophylactic DPPC coating through secondary lysosomal or extracellular
9 PLA-2 phospholipase enzymatic digestion restored the toxicity in 3-7 days [15,17-20,33,55]. These
10 differences were ascribed to variations in the rate of digestion by lysosomal enzymes.

11 It was emphasized in toxicology studies that critical toxic events in mineral dust-induced fibrosis occur in
12 cells in the alveolar interstitium rather than in the macrophages of the alveolar surface hypophase [56]
13 and investigations should also be carried out on pulmonary alveolar interstitial cells [19]. Sager [1]
14 reported that data from their laboratory indicate that improved dispersion of SWCNTs resulted in
15 significant enhanced potency of aspirated material to induce interstitial fibrosis in mice.

16 Apart from the damage of lysosomes by the phagocytized cytotoxic particles another important reaction
17 of the macrophages with particles is the production and release of reactive oxygen species (ROS). Hertog
18 [5,23] and Foucaud [24] employed DPPC concentrations which according to our calculations enabled
19 complete monolayer coverage of their studied hydrophobic NPs, SWCNT and CB respectively and
20 reported an improved particle dispersion which was considered the reason for the increased ROS
21 production in A549 cells and DCFT oxidation in MonoMac-6 human cells.

22 Numerous reported studies showed that dispersion of NPs (especially CNTs) is critical to their effective
23 distribution in the lung. In line with these studies, our results revealed that P25 NPs coated with a
24 complete DPPC bilayer become more hydrophilic and generate stable dispersions with an average
25 hydrodynamic diameter of 110-190 nm. Published TEM images of aluminum particles inside an
26 endosome of A549 cell from *in vivo* studies also showed NP aggregates with similar sizes (100-200 nm)
27 [27]. This emphasizes the importance of conditioning the NP surface in toxicology studies to mimic
28 pulmonary exposure more closely. Employing DPPC in concentrations which enable a complete coverage
29 of NPs is an important step in achieving this aim. The establishment of standard dispersion media and
30 protocols will enable researchers to achieve a degree of concordance and hence, could greatly benefit
31 nanotoxicology research.

4. Conclusions

1 The enthalpy of wetting includes two NP parameters highly relevant to toxicology, wettability and
2 surface area and along with surface charge can be used to predict their dispersability and stability in
3 aqueous fluids and consequently, their interaction with biological systems.

4 On titania P25 NPs, the adsorption of a complete DPPC bilayer has had the following critical effects:

- 5 1) Increased hydrophilicity of NPs and aided their dispersion in aqueous media.
- 6 2) Reduces the specific surface area of dry NPs;
- 7 3) Reduced the toxicity of NPs on A549 cells in 24 hour tests.

8 To mimic the *in vivo pulmonary* conditions more closely and enable the replication of the surfactant *in*
9 *vivo* action, nanotoxicology studies should employ the most abundant surface active component of the
10 lung surfactant, DPPC in a DPPC/NPs wt. ratio which enables complete coverage of NPs. Following this
11 testing strategy will hopefully lead to reaching consensus in cytotoxicity results.

12 The investigation of DPPC adsorption on P25 titania NPs has provided important information on their
13 wettability, charge and dispersability in biological fluids with consequences on the lung cells uptake and
14 toxicity. This study represents a first step in establishing a protocol for nanotoxicity testing and we
15 recommend similar tests to be carried out on hydrophobic NPs along with investigating the effect of the
16 relevant SPs on the DPPC adsorption and particle toxicity.

References

- 17 [1] T.M. Sager, D.W. Porter, V.A., Robinson, W.G. Lindsley, D.E. Schwegler-Berry and V. Castranova,
18 Improved method to disperse nanoparticles for *in vitro* and *in vivo* investigation of toxicity,
19 *Nanotoxicology*, 2007, 1(2), 118-129.
- 20 [2] A. Shvedova, T. Sager, A. Murray, E. Kisin, D. Poster, S. Leonard, D. Schwegler-Berry, V. Robinson and
21 V. Castranova, Critical issues in the evaluation of possible adverse pulmonary effects resulting
22 from airborne nanoparticles, in *Nanotoxicology: Characterization, Dosing and Health Effects*, ed.
23 N.A. Monteiro-Riviere and C.L. Tran, Informa Healthcare, New York, London 2007a, 225-236.
- 24 [3] P. Wick, P. Manser, L.K. Limbach, U. Dettlaff-Weglikowska, F. Krumeich, S. Roth, W.J. Stark and A.
25 Bruinink, The degree and kind of agglomeration affect carbon nanotubes toxicity, *Toxicol. Lett.*,
26 2007, 168(2), 121-131.
- 27 [4] D. Porter, K. Sriram, M. Wolfarth, A. Jefferson, D. Schwegler-Berry, M. Andrew and V. Castranova, A
28 biocompatible medium for nanoparticle dispersion, *Nanotoxicology*, 2008, 2(3), 144-154.
- 29 [5] E. Herzog, H.J. Byrne, A. Casey, M. Davoren, A.G. Lenz, K.L. Maier, A. Duschl, G.J. Oostingh, SWCNT
30 suppress inflammatory mediator responses in human lung epithelium *in vitro*, *Toxicology and*
31 *Applied Pharmacology*, 2009a, 234, 378-390.

- 1 [6] W.E. Wallace, M.J. Keane, D.K. Murray, W.P. Chisholm, A.D. Maynard and T. Ong, 'Phospholipid lung
2 surfactant and nanoparticle surface toxicity: Lessons from diesel soots and silicate dusts', *J.*
3 *Nanopart. Res.*, 2007b, 9, 23-38.
- 4 **[7] M.C. Bufford, R.F. Hamilton and A. Holian, A comparison of dispersing media for various engineering
5 carbon nanoparticles, *Particle and Fibre Toxicology*, 2007, 4(6), 1-9.**
- 6 [8] J.S. Patton, Mechanisms of macromolecule adsorption by the lungs, *Adv. Drug Deliv. Rev.*, 1996, 19, 3-
7 36.
- 8 [9] R. Veldhuizen, K. Nag, S. Orgeig and F. Possmayer, The role of lipids in pulmonary surfactant, *Biochim.*
9 *Biophys. Acta*, 1998, 1408, 90-108.
- 10 **[10] S. Schurch, P. Gehr, V.I. Hof, M. Geiser and F. Green, Surfactant displaces particles toward the
11 epithelium in airways and alveoli, *Respiration Physiology*, 1990, 80, 17-32.**
- 12 **[11] S. Schurch, H. Bachofen, J. Groeke and F. Green, Surface properties of rat pulmonary surfactant
13 studied with the captive bubble method: adsorption, hysteresis, stability, *Biochim. Biophys. Acta*,
14 1992, 1103, 127-136.**
- 15 **[12] W.R. Schief, M. Antia, B.M. Discher, S.B. Hall and V. Vogel, Liquid crystalline collapse of pulmonary
16 surfactant monolayers, *Biophys. J.*, 2003, 84, 3792-3806.**
- 17 **[13] F. Possmayer, Pulmonary Perspective. A Proposed Nomenclature for Pulmonary Surfactant-
18 associated Proteins, *Am. Rev. Respir. Dis.*, 1988, 138, 990-998.**
- 19 [14] W.E. Wallace, M.J. Keane, C.A. Hill, J. Xu and T.M. Ong, Mutagenicity of diesel exhaust particles and
20 oil shale particles dispersed in lecithin surfactant, *J. Toxicol. Environ. Health*, 1987, 21, 163-171.
- 21 [15] W.E. Wallace, M.J. Keane, V. Vallyathan, P. Hathaway, E.D. Regad, V. Castranova and F.H.Y. Green,
22 Suppression of Inhaled particles cytotoxicity by pulmonary surfactants and re-toxication by
23 phospholipase: distinguishing properties of quartz and kaolin, *Ann. Occup. Hyg., Inhaled Particles VI*,
24 1988, 32, 291-298.
- 25 [16] W.E. Wallace, M.J. Keane, P.S. Mike, C.A. Hill, V. Vallyathan and E.D. Regad, Contrasting respirable
26 quartz and kaolin retention of lecithin surfactant and expression of membranolytic activity following
27 phospholipase A2 digestion, *J. Toxicol. Environ. Health*, 1992, 37, 391-409.
- 28 **[17] C.A. Hill, W.E. Wallace, M.J. Keane and P.S. Mike, The enzymatic removal of a surfactant coating
29 from quartz and kaolin by P388D1 cells, *Cell Biol. Toxicol.*, 1995, 11, 119-128.**
- 30 **[18] X. Liu, M.J. Keane, J.C. Harrison, E.V. Cilento, T. Ong, W.E. Wallace, Phospholipid surfactant
31 adsorption by respirable quartz and in vitro expression of cytotoxicity and DNA damage,
32 *Toxicology Letters*, 1998, 96(97), 77-84.**

- 1 [19] N. Gao, M.J. Keane, T. Ong and W.E. Wallace, Effects of Simulated Pulmonary surfactant on the
2 cytotoxicity and DNA-Damaging activity of the respirable quartz and Kaolin, *J. of Toxicology and*
3 *Environmental Health*, 2000, Part A, 60, 153-167.
- 4 [20] N. Gao, M.J. Keane, T. Ong, J. Ye, W.E. Miller and W.E. Wallace, Effects of Phospholipid Surfactant
5 on Apoptosis Induction by Respirable Quartz and Kaolin in NR8383 rat pulmonary macrophages,
6 *Toxicology and Applied Pharmacology*, 2001, 175, 217-225.
- 7 [21] D.K. Murray, J.C. Harrison and W.E. Wallace, A 13C CP/MAS and 31P NMR study of the interactions of
8 dipalmitoylphosphatidylcholine with respirable silica and kaolin, *J. Colloid Interface Sci.*, 2005, 288,
9 166-170.
- 10 [22] W.E. Wallace, M.J. Keane, M. Guatam, X.C. Shi, D. Murray and T. Ong, Dispersion of nanoparticles
11 in pulmonary surfactants for in vitro toxicity studies: lessons from ultrafine diesel exhaust particles
12 and fine mineral dusts, in *Nanotoxicology: Characterization, Dosing and Health Effects*, ed. N.A.
13 Monteiro-Riviere and C.L. Tran, Informa Healthcare, New York, London 2007a, 153-172.
- 14 [23] E. Herzog, H.J. Byrne, M. Davoren, A. Casey, A. Duschl and G.J. Oostingh, Dispersion medium
15 modulates oxidative stress response of human lung epithelial cells upon exposure to carbon
16 nanomaterial samples, *Toxicology and Applied Pharmacology*, 2009b 236, 276-281.
- 17 [24] L. Foucaud, M.R. Wilson, D.M. Brown and V. Stone, Measurement of reactive species production by
18 nanoparticles prepared in biologically relevant media, *Toxicology Letters*, 2007, 174, 1-9.
- 19 [25] M. Ratoi, H.A. Spikes and H.L. Rieffe, Optimizing film formation by oil-in-water emulsions,
20 *Tribology Transactions*, 1997, 40(4), 569-578.
- 21 [26] B.P. Binks, L. Isa and A.T. Tyowua, Direct measurement of contact angles of silica particles in
22 relation to double inversion of pickering emulsions, *Langmuir*, 2013, 29, 4923-4927.
- 23 [27] K.W. Powers, S.C. Brown, V.B. Krishna, S.C. Wasdo, B.M. Moudgil and S.M. Roberts, Research
24 strategies for safety evaluation of nanomaterials. Part VI. Characterization of Nanoscale Particles
25 for Toxicological Evaluation, *Toxicological Sciences*, 2006, 90(2) 296-303.
- 26 [28] G.D. Parfitt and D.G. Wharton, The dispersion of rutile powder in aqueous surfactant solutions, *J.*
27 *of Colloid and Interf. Sci.*, 1972, 38, 2, 431-439.
- 28 [29] J.N. Israelachvili and G.E. Adams, Measurement of forces between 2 mica surfaces in aqueous
29 electrolyte solutions in range 0-100 nm, *Journal of the Chemical Society, Faraday Transactions*,
30 1978, 74, 1, 975-1001.
- 31 [30] F. Tiberg, Physical characterization of non-ionic surfactant layers adsorbed at hydrophilic and
32 hydrophobic solid surfaces by time-resolved ellipsometry, *J. Chem. Soc., Faraday Trans*, 1996, 92,
33 531-538.

- 1 [31] V. Oliynyk, U. Kaaze and T. Heimburg, Defect formation of lytic peptides in lipid membranes and
2 their influence on the thermodynamic properties of the pore environment, *Biochim et Biophysica*
3 *Acta*, 2007, 1768, 236-245.
- 4 [32] M. Kendall, T.D. Tetley, E. Wigzell, B. Hutton, M. Nieuwenhuijsen and P. Luckham, Lung lining liquid
5 modifies PM2.5 in favor of particle aggregation: a protective mechanism, *Am. J. Physiol. Lung Cell*
6 *Mol. Physiol.*, 2002, 282, L109-L114.
- 7 [33] J. Schimmelpfeng, E. Drosselmeyer, V. Hofheinz and A. Seidel, Influence of surfactant components
8 and exposure geometry on the effects of quartz and asbestos on alveolar macrophages, *Environ.*
9 *Health Perspect.*, 1992, 97, 225-231.
- 10 [34] T.D. Blake, Wetting, in *Surfactants*, ed. Th.F. Tadros, Academic Press, Harcourt Brace Jovanovich
11 Publ., 1984, ch.10, 221-276
- 12 [35] T. W. Healy and D. W., Fuerstenau, The oxide-water interface- interrelation of the zero point of
13 charge and the heat of immersion, *J. Coll. Sci.*, 1965, 20(4), 376-386.
- 14 [36] J. Geys, B. Nemery, P.H. Hoet, Assay conditions can influence the outcome of cytotoxicity tests of
15 nanomaterials: better assay characterization is needed to compare studies, *Toxicol. in Vitro.*, 2010,
16 24(2), 620-629.
- 17 [37] S. Lanone, F. Rogerieux, J. Geys, A. Dupont, E. Maillot-Marechal, J. Boczkowski, G. Lacroix and P.
18 Hoet, Comparative toxicity of 24 manufactured nanoparticles in human alveolar epithelial and
19 macrophage cell lines, *Part Fibre Toxicol.*, 2009, 6(14), 1-12.
- 20 [38] K. Suttiponparnit, J. Jiang, M. Sahu, S. Suvachittanont, T. Charinpanitkul and P. Biswas, Role of
21 surface area, primary particle size and crystal phase on titanium dioxide nanoparticle dispersion
22 properties, *Nanoscale Research Letters*, 2011, 6(27), 1-8.
- 23 [39] S. Ahmed and S.L. Wunder, Effect of High surface Curvature on the Main Phase Transition of
24 Supported Phospholipid Bilayers on SiO₂ Nanoparticles, *Langmuir*, 2009, 5, 3682-3691.
- 25 [40] L. Opilik, T. Bauer, T. Schmid, J. Stadler and R. Zenobi, Nanoscale Chemical Imaging of Segregated
26 Lipid Domains using Tip-Enhanced Raman Spectroscopy, *Phys. Chem. Chem. Phys.*, 2011, 13, 9978-
27 9981.
- 28 [41] E.N. Lewis, R. Bittman and I.W. Levin, Methyl group substitution at C(1), C(2) or C(3) of the glycerol
29 backbone of a diether phosphocholine: a comparative study of bilayer chain disorder in the gel and
30 liquid-crystalline phases, *Biochim et Biophysica Acta*, 1986, 861(1), 44-52.
- 31 [42] S. Ahmed, S.L. Wunder and Z.S. Nickolov, 'Raman Spectroscopy of Supported Lipid Bilayer
32 Nanoparticles', *Spectroscopy*, 2011, Special Issues, June
33 <http://www.spectroscopyonline.com/spectroscopy/article> retrieved on 30th October 2013.

- 1 [43] J.M. Douillard, J. Zajac, Contact Angle Determination from Heat of Immersion and Heat of Wetting, in
2 *Encyclopedia of Surface and Colloidal Science*, ed. P. Somasundaran, Marcel Dekker, New York,
3 Update Supplement, 2004, 153-163.
- 4 [44] G. Buckton, Characterization of small changes in the physical properties of powders of significance
5 for dry powder inhaler formulations, *Advanced drug delivery reviews*, 1997, 26, 17-27.
- 6 [45] Y.W. Yang, G. Zografi and E.E. Miller, Capillary flow phenomena and wettability in porous media II.
7 Dynamic flow studies, *J. Colloid Interface Sci.*, 1988, 122, 35-46.
- 8 [46] R.M. Shanker, P.J. Baltusis and R.M. Hruska, Development of a new technique for the assessment
9 of wettability of powders, *Pharm. Res.*, 1995, 11, s-243.
- 10 [47] T.N. Hunter, G.J. Jameson and E.J. Wanless, Determination of contact angles of nanosized silica
11 particles by multi-angle single-wavelength ellipsometry, *Aust. J. Chem.*, 2007, 60, 615-655.
- 12 [48] L. Isa, F. Lucas, R. Wepf and E. Reimhult, Measuring single-nanoparticle wetting properties by
13 freeze-fracture shadow-casting cryo-scanning electron microscopy, *Nature Communications*, 2011,
14 2(438), 1-9.
- 15 [49] D.W. Fuerstenau and S. Raghavan, Some aspects of flotation thermodynamics. In M.C Fuerstenau,
16 G. Jameson and R.-H. Yoon, (Eds.), *Froth Flotation, A Century of Innovation*, 2007, Society of
17 Mining, Metallurgy and Exploration (SME), Colorado, USA, 95-132.
- 18 [50] M. Jurak and E. Chibowaki, Wettability and topography of phospholipid DPPC multilayers
19 deposited by spin-coating on glass, silicon and mica slides, *Langmuir*, 2007, 23, 10156-10163.
- 20 [51] K.J.A. Raj and B. Viswanathan, Effect of surface area, pore volume and particle size of P25 titania on
21 the phase transformation of anatase to rutile, *Indian Journal of Chemistry*, 2009, 48A, 1378-1382.
- 22 [52] S. Patzold, A. Schmidt, A. Seidel, Loss of cathepsin B activity in alveolar macrophages after in vitro
23 quartz phagocytosis, *J. Toxicol. Environ. Health*, 1993, 40, 547-554.
- 24 [53] J.M. Antonini and M.J. Reasor, Effect of short-term exogenous pulmonary surfactant treatment of
25 acute lung damage associated with the intratracheal instillation of silica, *J. Toxicol Environ Health*,
26 1994a, 43, 85-101.
- 27 [54] J. Bignon and M.C. Jaurand, Biological *in vitro* and *in vivo* responses of chrysotile versus
28 amphiboles, *Environ. Health Perspect.*, 1983, 51, 73-80.
- 29 [55] J.M. Antonini, C.M. McCloud and M.J. Reasor, Acute silica toxicity: attenuation by amiodarone-
30 induced pulmonary phospholipidosis, *Environ. Health Perspect.*, 1994b, 102, 372-378.
- 31 [56] I.Y.R. Adamson, H.L. Letourneau and D.H. Bowden, Enhanced macrophage-fibroblast interactions in
32 the pulmonary interstitium increase fibrosis after silica injection to monocyte-depleted mice, *Am. J.*
33 *Physiol.*, 1989, 134, 411-417.